ISSN: 2414-1895 DOI: 10.6919/ICJE.202505_11(5).0053

Static Analysis and Optimization of the Cabin Structure of the Safety Refuge Device

Yong Wang[1, *], Junhao Song[1], Kunpeng Xing[1], Degong Chang[2], Xiumin Jing[2]

[1] School of Science, Qingdao University of Technology, Qingdao, 266525, Shandong, PR China

[2] College of Electromechanical Engineering, Qingdao University of Science and Technology, Qingdao, 266061, Shandong, PR China

*Corresponding Author: wang_yong@qut.edu.cn

Abstract

Aiming at the technical problems of pressure resistance, explosion resistance and structural optimization of the safety refuge device, the cabin structure of the safety refuge device was parametrically modeled, and a new triangular cabin structure model was established. Loads were applied to the established triangular cabin, and static analysis was performed using ANSYS Workbench to observe the stress and deformation distribution of the cabin. Taking the quasi-triangular cabin structure as the research object, the optimized mathematical model of the cabin is established, and the equivalent stress, total deformation and quality of the quasi-triangular cabin are multi-objective optimized by using Creo and AWE joint simulation. The optimal solution of the quasi-triangular cabin structure is found through DOE optimization method. The analysis results show that: under the premise of unchanged cabin mass, the optimized cabin stress and total deformation are relatively reduced a lot, achieving the purpose of cabin optimization design, meeting the overall design requirements of the safety refuge device, and providing effective theoretical basis and technical support for the design and manufacture of the safety refuge device.

Keywords

The Safety Refuge Device; Quasi-Triangular Cabin; Static Analysis; Optimization Design.

1. Preface

The safety shelter is an escape device, which is an enclosed cabin structure that can provide emergency shelter and protect the lives of disaster victims in the event of a sudden disaster or catastrophe [1-2]. Foreign countries started research on safety shelter devices early and developed some emergency escape devices. The "Tsunami Safety Emergency Shelter" was jointly developed by Japanese scientists and the American company Survival Capsule LLC [3]. This spherical safety emergency shelter can be used to shelter people in case of an impending tsunami. Argentina's escape box is composed of two parts: a cogwheel and a single track, with several small boxes for people attached to the track. This device can evacuate people quickly [4]. Domestic research on safety shelters started late, lacks experience and experimental support, and related technical standards need to be improved. Chang Degong, Li Songmei, Jing Xiumin and others from Qingdao University of Science and Technology conducted structural design and fall impact resistance research on urban emergency shelters to solve the problem of safe refuge for people escaping from high-rise buildings during disasters, and proposed a new structural model for urban emergency shelters [5-6]. Wang Yong and others from Qingdao University of Technology took urban safety emergency shelters as the research object, drew on the design and research ideas of mining safety emergency shelters,

ISSN: 2414-1895 DOI: 10.6919/ICJE.202505_11(5).0053

designed and studied the cabin structure of urban safety emergency shelters, and designed the overall structure of the cabin door of the shelter [7-10]. Shanxi Chongsheng Mining Technology Co., Ltd. and the University of Science and Technology Beijing jointly carried out a national science and technology support project and developed a prototype of a mine rescue capsule [11-12]. They also conducted real-life survival simulation tests and gas explosion resistance tests. Wang Yuanbin and Xu Dehua from Southwest Jiaotong University proposed a design for an earthquake-resistant lifeboat, put forward a preliminary concept for the earthquake-resistant performance design of the lifeboat, and conducted theoretical and experimental analysis on its reliability [13].

Based on the pressure resistance performance of the safety refuge device, this paper parametrically models the cabin structure of the safety refuge device and establishes a new triangular cabin structure model. Loads were applied to the established triangular cabin, and static analysis was performed using ANSYS Workbench to observe the stress and deformation distribution of the cabin. Taking the triangular cabin structure as the research object, an optimized mathematical model of the cabin is established. The equivalent stress, total deformation and mass of the triangular cabin are optimized by multi-objective design using Creo and AWE joint simulation. The optimal solution of the triangular cabin structure is found through DOE optimization method, which provides an effective theoretical basis and technical support for the design and manufacture of safe shelters.

2. Parametric Modeling of Cabin Structure

This paper first establishes a triangular cabin structure model, as shown in Figure 1, and then conducts parametric design based on it.

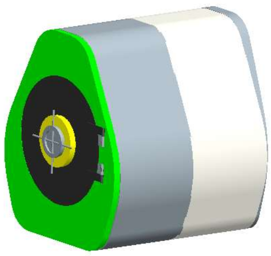

Figure 1. Triangular cabin structure model

Table 1. Initial values and upper and lower limits of parameters of triangular cabin structure

parameter	DS_1/mm	DS_2/mm	DS_3/mm	DS_4/mm	DS_5/mm	DS_6/mm	DS_7 /mm
Initial value	200	260	700	220	12	45	20
Upper limit	180	245	685	210	10	42	22
Lower limit	210	275	710	230	14	48	28

Parametric modeling uses parameter modification and function relationship setting to adjust the model size, avoiding the problem that the model cannot be optimized and analyzed due to fixed size [14]. In addition, the parametric modeling setting of DM is used to facilitate batch processing of data established by multiple sets of sub-parameter comparison numerical simulations. When optimizing the cabin structure, it is necessary to first perform parametric modeling on the cabin structure. The main factors affecting the strength of the safety shelter include: the upper top of the cabin (DS_1), the upper transition fillet (DS_2), the middle transition fillet (DS_3), the lower transition fillet (DS_4), the length of the transverse (longitudinal) reinforcement rib (DS_6), the width of the transverse (longitudinal) reinforcement rib (DS_7), and the thickness of the cabin (DS_5), etc. Therefore, it is used as the design variable, and the initial value and upper and lower limits of the design variable are set as shown in Table 1.

3. Static Analysis of Cabin

3.1 Apply Loads and Constraints to the New Model

According to the general technical requirements for mine safety refuge devices, the cabin must meet the pressure resistance requirement of 0.3 MPa or higher [15-16]. The pressure resistance of the cabin structure of the safety refuge device is designed to be 0.3MPa, that is, a stress of 0.3MPa is applied to the entire outer surface of the cabin, which is added through Pressure in Static Structure. Considering the size of the high-rise residential building, a fixed constraint is applied to the bottom surface of the entire cabin structure through Fixed Support [17]-[18]. The specific loads and constraints are shown in Figure 2.

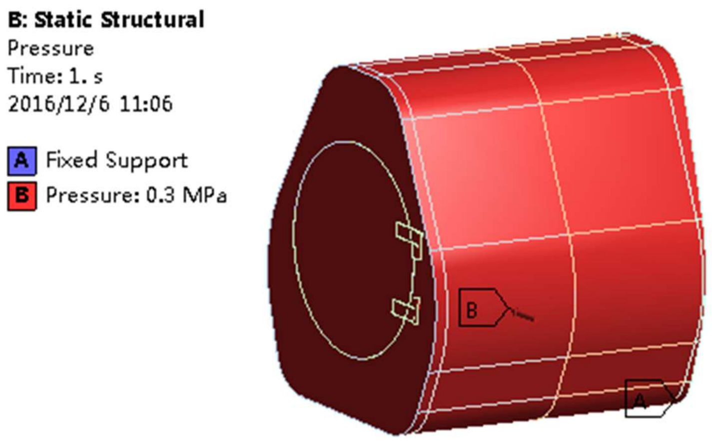

Figure 2. Applied load and constraint diagram for a triangular-shaped cabin

3.2 Simulation Results of Triangular Cabin

The equivalent stress and total deformation cloud diagrams obtained after solving the overall structure of the safety refuge device are shown in Figures 3 and 4.

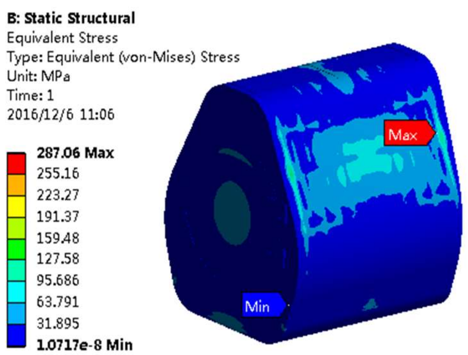

Figure 3. Equivalent stress cloud diagram

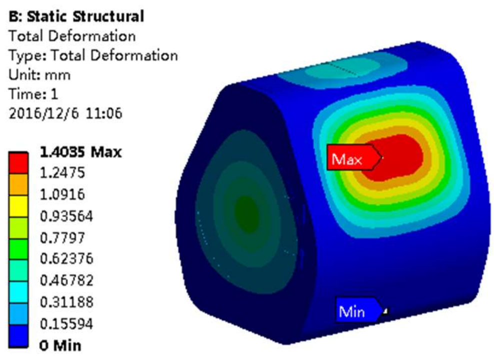

Figure 4. Total deformation cloud map

As can be seen from Figures 3 and 4, the maximum stress occurs on the side of the cabin, with a maximum stress of 287.06MPa. The obvious deformation sites are located on the side of the cabin shell, on the front door of the cabin, and on the upper surface of the cabin shell, with deformations of 1.4035mm, 0.93564mm, and 0.62376mm respectively.

4. Optimization Analysis of Triangular Cabin Structure

4.1 Optimization Mathematical Model

In this paper, the obtained equivalent stress *σ(X)*, total deformation *s(X)* and cabin mass *m(X)* are set as optimization targets and optimized to improve the overall performance of the cabin structure of the safety shelter.

The mathematical model for cabin optimization analysis is established as follows:

$$\begin{cases} \min F(X)=\min(\sigma(X),s(X),m(X))^T \\ 180\le g_1(X)=DS\_1\le 210 \\ 245\le g_2(X)=DS\_2\le 275 \\ 685\le g_3(X)=DS\_3\le 710 \\ 210\le g_4(X)=DS\_4\le 230 \\ 10\le g_5(X)=DS\_5\le 14 \\ 42\le g_6(X)=DS\_6\le 48 \\ 22\le g_7(X)=DS\_7\le 28 \\ X=(x_1,x_2,x_3)^T=(DS\_1,DS\_2,DS\_3,DS\_4,DS\_5,DS\_6,DS\_7)^T \end{cases} \tag{1}$$

In the formula:

F(X)- Objective Function;

Gi(X)- State variables;

X- Design variables;

DS_i- parameter.

4.2 Optimize Settings

In the Geometry of the safety shelter, the above 7 parameters are activated and used as input parameters, that is, DS_1 in Creo software corresponds to P1 in Workbench, DS_2 corresponds to P7, DS_3 corresponds to P6, DS_4 corresponds to P5, DS_5 corresponds to P4, DS_6 corresponds to P3, and DS_7 corresponds to P2. In the model, activate the cabin mass P10, and in the Result, activate the maximum equivalent stress P8 and the maximum deformation P9 as output functions, and insert the optimization module.

4.3 Analysis of Optimization Results of Triangular Cabin

Set the upper and lower limits of the parameters to the same values as those set in Section 2, update the parameters in Design of Experiments, and obtain 80 sets of design points. Each time a set of design points is retrieved, the model must be adjusted and then the static analysis must be performed again, and the entire iterative process is completed through cycles and iterations. The response surface relationship and design curve relationship between each input parameter and output parameter (i.e., objective function) are displayed through the Response Point command under Response Surface in the optimization module, as shown in Figures 5, 6, 7, and 8.

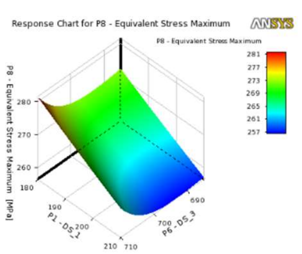

(a) Response surface of P1, P6 and P8

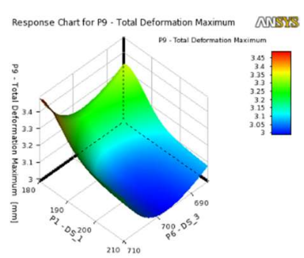

(b) Response surface of P1, P6 and P9

ISSN: 2414-1895 DOI: 10.6919/ICJE.202505_11(5).0053

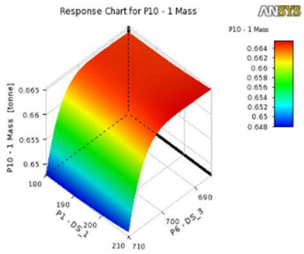

(c) Response surface of P1, P6 and P10

Figure 5. Response surface relationship between P1, P6 and output parameters

From (a), (b) and (c) in Figure 5, we can see the relationship between the cabin top P1, the middle transition fillet P6 and the objective function. Figure (a) shows the relationship between the parameters P1, P6 and the equivalent stress P8. As P1 increases, the maximum equivalent stress decreases gradually; as P6 increases, the maximum equivalent stress increases. Figure (b) shows the relationship between the parameters P1, P6 and the total deformation P9. As P1 increases, the total deformation P9 decreases gradually; as P6 increases, the total deformation P9 increases. Figure (c) shows the relationship between parameters P1, P6 and mass P10. As P1 increases, mass P10 tends to increase gradually; as P6 increases, mass P10 tends to decrease. Since the goal is to obtain the minimum value of the maximum equivalent stress and maximum deformation of the cabin, supplemented by the minimum value of the cabin's mass, when selecting the optimal solution later, a larger value of P1 and a smaller value of P6 should be selected as much as possible.

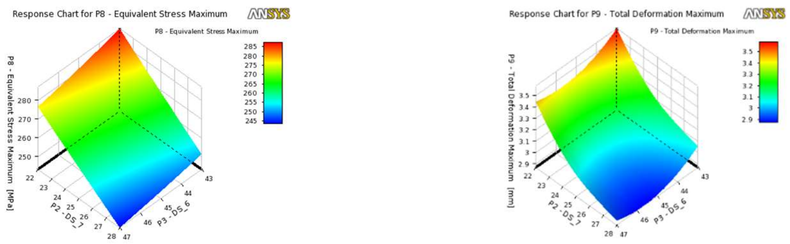

(a) Response surface of P2, P3 and P8 (b) Response surface of P2, P3 and P9

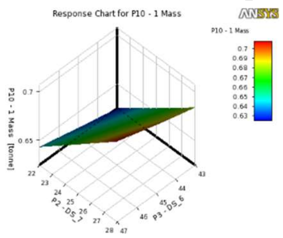

(c) Response surface of P2, P3 and P10

Figure 6. Response surface relationship between P2, P3 and output parameters

From (a), (b) and (c) in Figure 6, we can see the relationship between the width P2 of the transverse (longitudinal) reinforcement rib, the length P3 of the transverse (longitudinal) reinforcement rib and the objective function. Figure (a) shows the relationship between the input parameters P2, P3 and the equivalent stress P8. As P2 increases, the maximum equivalent stress P8 decreases gradually. As P3 increases, the maximum equivalent stress P8 also decreases gradually. Figure (b) shows the relationship between parameters P2, P3 and total deformation P9. As P2 increases, total deformation P9 decreases gradually. As P3 increases, total deformation P9 also decreases gradually. Figure (c) shows the relationship between parameters P2, P3 and mass P10. As P2 increases, mass P10 tends to increase gradually; as P3 increases, mass P10 tends to increase. Since the goal is to obtain the minimum value of the maximum equivalent stress and maximum deformation of the cabin,

ISSN: 2414-1895 DOI: 10.6919/ICJE.202505_11(5).0053

supplemented by the minimum value of the cabin's mass, when selecting the optimal solution later, larger values of P2 and P3 should be selected as much as possible.

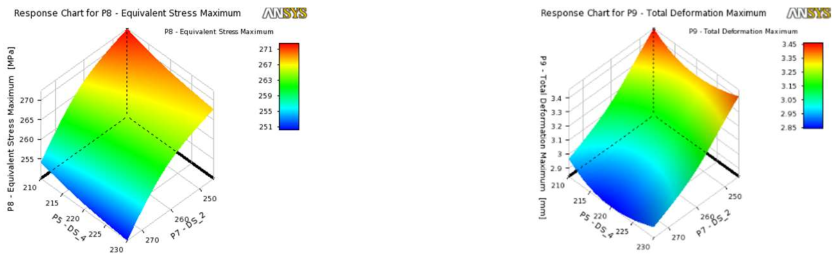

(a) Response surface of P5, P7 and P8 (b) Response surface of P5, P7 and P9

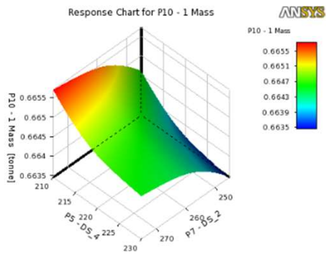

(c) Response surface of P5, P7 and P10

Figure 7. Response surface relationship between P5, P7 and output parameters

From (a), (b) and (c) in Figure 7 , it can be seen that the changing relationship between the upper transition fillet P7, the lower transition fillet P5 and the objective function. Figure (a) shows the relationship between parameters P5, P7 and equivalent stress P8. As P5 increases, the maximum equivalent stress P8 decreases gradually. As P7 increases, the maximum equivalent stress P8 also decreases gradually. Figure (b) shows the relationship between parameters P5, P7 and total deformation P9. As P5 increases, total deformation P9 decreases gradually. As P7 increases, total deformation P9 also decreases gradually. Figure (c) shows the relationship between parameters P2, P3 and mass P10. As P5 increases, mass P10 decreases gradually; as P7 increases, mass P10 increases. Since the goal is to obtain the minimum value of the maximum equivalent stress and maximum deformation of the cabin, supplemented by the minimum value of the cabin's mass, when selecting the optimal solution later, larger values of P5 and P7 should be selected as much as possible.

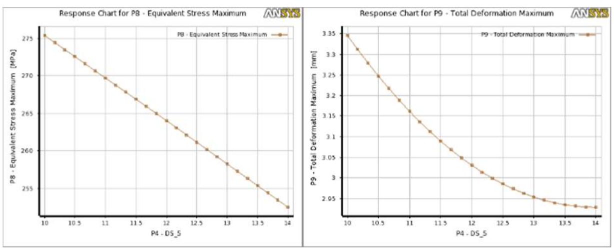

(a) Design curves of P4 and P8 (b) Design curves of P4 and P9

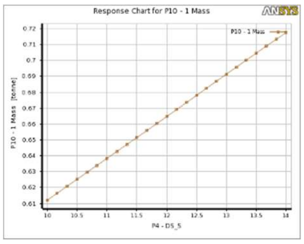

(c) Design curves of P4 and P10

Figure 8. Relationship between P4 and output parameter design curve

From (a), (b) and (c) in Figure 8, we can clearly see the linear relationship between the cabin thickness P4 and the objective function. Figure (a) shows that as P4 increases, the maximum equivalent stress P8 tends to decrease gradually, ranging from 275Mpa to 252Mpa; Figure (b) shows that as P4 increases, the total deformation P9 tends to decrease gradually, and the maximum deformation ranges from 3.3mm to 2.9mm; Figure (c) shows that as P4 increases, the mass P10 gradually increases, with the minimum mass being 0.612t and the maximum mass being 0.72t. Since the goal is to obtain the minimum value of the maximum equivalent stress and maximum deformation of the cabin, supplemented by the minimum value of the cabin's mass, when selecting the optimal solution later, a larger value of P4 should be selected as much as possible.

From the above Figures 5, 6, 7 and 8, we can see the influence of various input parameters of the cabin on the output parameters. In terms of the degree of influence on the quality, the thickness P4 of the cabin has the greatest impact on the quality of the cabin. Other parameters such as the length P3 and width P2 of the stiffener also have a certain influence on the quality, but it is relatively small. In terms of the influence on the equivalent stress, P2 and P4 have a relatively large influence on the stress of the cabin, and other parameters such as P1 and P7 have a smaller influence; In terms of the influence on the total deformation, P2 has the greatest impact on the total deformation of the cabin, while other parameters such as P7 and P4 have relatively smaller effects. In terms of the importance of influencing each output parameter, the stiffener affects the stress and total deformation of the cabin, while the thickness of the cabin affects the mass of the cabin.

After the calculation of the 80 sets of optimized and updated design points is completed, a set of selected points that best meet the requirements is obtained, and the model size is changed to the value of this selected point in Creo. The static analysis of the cabin structure of the safety refuge device is carried out to obtain the new maximum equivalent stress and maximum deformation. The comparison results between the new design point and the initial design point are shown in Table 2.

Table 2. Comparison of parameters before and after optimization

parameter	Before optimization	After optimization	Change
P1/(mm)	200	204.95	
P2/(mm)	20	27.927	
P3/(mm)	45	43.761	
P4/(mm)	12	11.066	
P5/(mm)	220	226.88	
P6/(mm)	700	700.62	
P7/(mm)	260	274.71	
P8 Maximum stress value /(MPa)	287.06	233.84	-18.5%
P9 Maximum deformation /(mm)	3.4506	2.9584	-14.3%
P10 quality /(t)	0.6972	0.66273	-0.05%

It can be seen from Table 2 that after optimizing the cabin, the indicators of the cabin's output parameters have all decreased; Under the premise that the mass of the cabin remains unchanged, the stress and total deformation of the cabin are relatively reduced a lot, achieving the purpose of cabin optimization design and meeting the overall design requirements of the safety shelter.

5. Conclusion

This paper proposes a new type of triangular safety refuge device, parametrically models it through Creo, and performs static analysis on the triangular cabin in the Static Structure module in ANSYS Workbench to obtain the distribution of equivalent stress and total deformation. A mathematical model for optimization analysis of the triangular safety shelter was established, and the equivalent stress, total deformation and mass of the triangular cabin were optimized by joint simulation of Creo and AWE. A set of points that best met the requirements of the triangular cabin structure was found through DOE optimization method. Under the premise that the mass of the cabin remains unchanged, the stress and total deformation of the optimized cabin are relatively reduced a lot, achieving the purpose of cabin optimization design, meeting the overall design requirements of the safety refuge device, and providing an effective theoretical basis and technical support for the design and manufacture of the safety refuge device.

Acknowledgments

Funding: This work was supported by the Qingdao Natural Science Foundation (24-4-4-zrjj-80-jch).

Data Availability Statement

The data used to support the findings of this study are available from the corresponding author upon request.

Conflicts of Interest

The authors declare that there are no conflicts of interest regarding the publication of this article.

References

[1] DONG B Y, ZHANG Z Q, XU L J, et al. Research status and development trend of intelligent emergency rescue equipment[J]. Journal of Mechanical Engineering,2020, 56(11):1-25.

[2] LUO H S, DOU H Y, DAI Z, et al. Simulation and verification of the scaled model of the rescue capsule under impact load[J]. Safety in Coal Mines,2021, 52(12):7.

[3] SAMANTA B K. Geotechnical Challenges in World Record Making Mine Rescue[C]//International Conference on Geotechnical Challenges in Mining, Tunneling and Underground Infrastructures. Springer, Singapore,2022.

[4] ZHANG L, KONG B, LIN S Y, et al. Research on the vibration-absorptive design of the independent escape capsule[J]. Ocean Engineering,2021, 39(2):179-195.

[5] LI S M, JING X M, WANG Y, et al. Analysis of drop impact of urban emergency shelters[J]. Journal of Mechanical & Electrical Engineering,2017, 219:108296.

[6] JING X M. Structural design and analysis of a new type of domestic lifeboat[D]. Qingdao: Qingdao University of Science and Technology,2017:54-57.

[7] WANG Y. Design and research of urban safety emergency shelter[D]. Qingdao: Qingdao University of Science and Technology,2018:64-67.

[8] WANG Y, WANG Y Y, LI S M, et al. Research on the Novel Honeycomb-Like Cabin Based on Computer Simulation[J]. Computer Systems Science and Engineering,2021, 39(2):179-195.

[9] WANG Y, WANG Y Y, CUI L Z, et al. The seismic analysis of the safety evacuation device[C]//IOP Conference Series Earth and Environmental Science. 2019,384:012230.

[10] WANG Y, FENG X Z, CUI L Z, et al. The explosion resistance analysis of the safety evacuation device[C]//IOP Conference Series: Materials Science and Engineering. 2020,772(1):012104.

[11] CHEN X K, LI H T, WANG Q H, et al. Explosion resistance analysis and structural optimization of mining cylindrical shell rescue cabin under gas explosion load[J]. Explosion and Shock Waves,2018, 38(01):124-132.

[12] XU P, FAN Z H, YU Y H, et al. Analysis on collision and sound insulation performance of circular foam aluminum composite structure lifeboat[J]. Journal of Safety and Environment,2022, 22(01):123-131.

[13] WANG Y B, XU D H, et al. Research on the development and application of an earthquake-resistant life-saving facility[J]. Science & Technology Information,2012, 11:216.

[14] BAI X Y, LI A, YAO X G, et al. Research on parametric design method based on Pro/E behavior modeling method[J]. Journal of Mechanical & Electrical Engineering,2020, 37(03):307-310.

[15] MENG H, HE X M, et al. Research on the design of mining rescue capsule based on integrated innovation theory[J]. Industrial Design,2020, 1:2.

[16] MA L, LIU S, WEI G, et al. Dynamic Response Characteristics of a Sealing Airbag under Different Impact Types and Impact Pressures[J] ACS omega,2022,7(43):38589-38599.

[17] ZHANG L, KONG B, LIN S, et al. Fluid-structure interaction problem of hydrodynamic motion of an independent escape capsule under variable constraint conditions[J]. Ocean Engineering,2019, 187:106198.1-106198.17.

[18] WANG F, LI Y J, HE Z H, et al. The Ultimate Strength of Fully Transparent Pressure-Resistant Spherical Cabins[J]. Applied Sciences,2023,13(22):12229.